

**A MASTER CURVE ANALYSIS OF F82H USING STATISTICAL AND CONSTRAINT LOSS SIZE ADJUSTMENTS OF SMALL SPECIMEN DATA**—G. R. Odette, T. Yamamoto, H. Kishimoto, W. J. Yang, and G. E. Lucas (University of California, Santa Barbara), M. Sokolov (Oak Ridge National Laboratory), P. Spätig (CRPP EPFL, Switzerland), and J.-W. Rensman (NRG Petten, The Netherlands)

## OBJECTIVE

The objective of this work was to assemble a database on the fracture toughness of the IEA heat of F82H normalized and  $\approx$  8Cr tempered martensitic steel and to assess the consistency of the data with the master curve method of establishing unirradiated reference toughness temperature curves.

## SUMMARY

We assembled a fracture toughness database for the IEA heat of F82H based on a variety of specimen sizes with an ASTM E1921 nominal master curve (MC) reference temperature,  $T_o = -119 \pm 3^\circ\text{C}$ . However, the data are not well represented by a MC.  $T_o$  decreases systematically with a decreasing deformation limit  $M_{lim}$  starting at  $\approx$  200, which is much higher than the E1921 censoring limit of 30, indicating large constraint loss in small specimens. The small scale yielding  $T_o$  at high  $M_{lim}$  is  $\approx -98 \pm 5^\circ\text{C}$ . While, the scatter is somewhat larger than predicted, after model-based adjustments for the effects of constraint loss, the data are in reasonably good agreement with a MC with a  $T_o = -98^\circ\text{C}$ . This supports to use of MC methods to characterize irradiation embrittlement, as long as both constraint loss effects are properly accounted for. Finally, we note various issues, including sources of the possible excess scatter, which remain to be fully assessed.

## PROGRESS AND STATUS

### Introduction

One of the key challenges facing the development of  $\approx$  8Cr normalized and tempered martensitic steels (TMS) for fusion applications is irradiation embrittlement. Embrittlement is best characterized in terms of fracture toughness-temperature curves,  $K_{Jc}(T)$ . Measuring fracture toughness requires pre-cracked specimens subject to strict size and geometry requirements. Various versions of the master curve (MC) method, described in the next section [1-4], greatly reduce fracture toughness testing requirements in terms of both the size and number of specimens. This is critical since embrittlement depends on the combination of a large number of variables and there are very severe restrictions on irradiation volumes that can be accessed, particularly at high dose and with good control of specimen temperatures.

However, use of small specimens demands that the issue of size effects be addressed directly [1,3,5-11]. The sources of such size effects and approaches to accounting for them are described in the next section. We focus on the issue of determining a toughness temperature curve,  $K_{Jr}(T)$ , for the IEA F82H reference heat. Previous studies suggested that there was considerable variability in the  $K_{Jr}(T)$  data for this heat, presumably associated with heterogeneities in the underlying microstructure, suggesting that a single MC can not represent IEA F82H. However, size effects were not fully assessed in the previous studies, confounding this conclusion. In order to evaluate the applicability of the MC method to TMS, a physically based method is used to adjust for size effects in the IEA F82H database and we assess the agreement of the adjusted data with a single MC.

### Background, Master Curve and Specimen Size and Geometry Effects on Fracture Toughness

Various MC methods *assume* there is a universal invariant toughness temperature curve shape,  $K_{Jc}(T - T_o)$ , or small family of shapes, in the cleavage transition regime that can be indexed on an absolute temperature (T) scale by a reference temperature ( $T_o$ ) at a median reference toughness of  $100 \text{ MPa}\sqrt{\text{m}}$  [1-4]. The American Society for Testing and Materials (ASTM) E1921 Standard MC is given by [2]

$$K_{Jc}(T-T_o) = 30 + 70[0.019(T-T_o)] \text{ (MPa}\sqrt{\text{m)}}. \quad (1)$$

$T_o$  can be measured using a relatively small number of relatively small specimens. The Master Curve-Shifts Method (MC- $\square T$ ) [1,3], adjusts the reference  $T_o$  for the alloy in the unirradiated condition with a set of temperature shifts ( $\square T_o$ ) to account for the loading rate [1] and irradiation embrittlement [1,3,4,6]. The effects of specimen size and geometry can also be treated in terms of a  $\square T_o$  and adjusted MC shapes [1,3,5]. Large  $\square T_o$  may control the lifetime of fusion reactor structures. However, the  $\square T_o$  that accounts for shallow surface cracks in thin-walled structures has a large negative value, thus may mitigate the effects of embrittlement [3].

The various  $\square T_o$  can be independently measured and modeled. For example, at irradiation temperatures below about 400°C, the  $\square T_o$  for embrittlement can be related the irradiation hardening, measured in tensile ( $\square \sigma_y$ ) or microhardness tests [1,4,6]. Further, models that relate  $\square \sigma_y$  to metallurgical and irradiation variables derived from fits to the large tensile test database can also be used to help model  $\square T_o$  [1,3,4,6]. Multiscale models can also be used to relate  $\square \sigma_y$ , hence  $\square T_o$ , to irradiation-induced microstructural evolutions, as well as to guide the development of radiation resistant alloys [3].

There is a large and growing body of data on the fracture toughness of TMS in the unirradiated and, to a lesser extent, irradiated conditions. However, these data represent a wide range of test specimen sizes and types [10-14]. Size and specimen geometry are known to influence the measured values of fracture toughness,  $K_{Jm}$ . Indeed, fracture toughness is an intrinsic, geometry and size-independent material property,  $K_{Jr}$ , only for very restricted reference conditions of a cracked-body (specimen or structure). Thus in order to assess the applicability of the MC method to TMS, it is necessary to properly account for size/geometry effects and to develop methods to transfer the measured  $K_{Jm}$  data to the intrinsic property at a reference condition,  $K_{Jr}$  (1,3,5-11), as well as to transfer the  $K_{Jr}$  to conditions pertinent to a cracked structure [1,3].

Two different size-effects must be considered. Constraint loss (CL) effects occur when the specimen ligament length,  $b$ , and/or thickness,  $B$ , are no longer small with respect to the dimension of the plastic zone of the crack [1,3,5-11]. Note that the ligament length is defined as  $b = W - a$ , where  $a$  is the crack length and  $W$  is the width of the specimen. Tri-axial constraint elevates the normal stress near the crack tip,  $\square_{22}$ , to values of 3 to 5 times  $\sigma_y$ . Any CL lowers  $\square_{22}$ , hence, a higher  $K_{Jm}$  is needed for cleavage fracture compared to the  $K_{Jc}$  for plane strain, deeply cracked specimens, loaded in bending under small-scale yielding (SSY) conditions.

$K_{Jm}$  and  $K_{Jc}$  also increase with a decreasing volume of material under the high  $\square_{22}$  stress field near a crack tip [2,3,7-9]. This derives from the fact that cleavage occurs when a critical  $\square_{22} = \square^*$  encompasses a sufficient volume of material to cause the formation and propagation of a microcrack from a broken, brittle trigger-particle, like a large grain boundary carbide. The trigger-particles have statistical size and spatial distributions; hence, they act in a way that is similar to a distribution of the strengths of the links in a long chain. Thus, cleavage is a statistical, weakest-link process, and this has two important consequences. The first is that there is an inherently large specimen-to-specimen scatter in  $K_{Jm}$  and  $K_{Jc}$ . Second, as noted above,  $K_{Jm}$  and  $K_{Jc}$  increase as the specimen thickness or crack front length,  $B$ , hence stressed volume, decreases. We refer to this as the statistical stressed volume (SSV) effect. The stressed volume scales with  $BK_J^4$  under SSY conditions.

In order to decouple the SSV from CL effects, we recently carried out a single-variable experiment on a large matrix of  $a/W \approx 0.5$ , 3-point bend specimens, with a wide range of  $B$  (8 to 254mm) and  $W$  (6 to 50 mm) [3,7-9]. The pre-cracked specimens were fabricated from a large plate section of the unused Shoreham A533B reactor pressure vessel. Eight specimens were tested at  $T = -91^\circ\text{C}$  and a constant loading rate for each  $B$ - $W$  combination. The baseline  $B$ - $W$  matrix was complimented by a large number of fracture tests using 1T compact tension and pre-cracked full and sub-sized Charpy specimens, as well as small bend bars with shallow,  $a/W \approx 0.2$ , pre-cracks. Tensile tests and optical metallography were also

carried out to characterize the constitutive properties and basic microstructure of the steel; and the fracture surfaces were characterized by scanning electron microscopy.

The B-W database showed that CL occurs at loading levels well below the current E1921 censoring limit, defined at  $M = b\sigma_y E'/K_{Jm}^2 > M_{lim} = 30$  [2]. However, the data also clearly show a SSV effect that is reasonably consistent with the scaling law in E1921 [2],

$$K_{Jr} = (K_{Jc} - K_{Jmin})(B/B_r)^{-1/4}. \quad (2)$$

Here  $B_r$  is a reference thickness of 25.4 mm. This expression reflects the stressed volume scaling as  $BK_J^4$ , modified by the assumption that cleavage only occurs above a minimum  $K_{Jmin}$ , taken as 20 MPa $\sqrt{m}$  in E1921 [2].

The single-variable B-W database was successfully analyzed with calibrated micromechanically-based three-dimensional (3D) finite element (FE) CL models [7-9]. The models were used to separate CL and SSV effects. The models compute the theoretical ratio of the large-scale yielding (LSY) to SSV loading ratio,  $[K_{Isy}/K_{Ssy}]$ , that produce the same local crack tip stress field conditions. One model was based on a local fracture criterion that assumes that cleavage occurs when the  $\sigma_{22} = \sigma^*$  stress contour encompasses a critical average in-plane area,  $A^*$ , of the fracture process zone in front of the crack tip. The model was used to evaluate  $[K_{Isy}/K_{Ssy}]$  for the Shoreham steel constitutive law as a function of  $B/W$ ,  $b$ ,  $\sigma^*/\sigma_y$  and  $K_{Isy}$ , where  $K_{Jc} = K_{Jm}/[K_{Isy}/K_{Ssy}]$  is evaluated at  $K_{Isy} = K_{Jm}$ . The calibration of  $\sigma^*$  involved fitting a  $\sigma^*-A^* K_{Jc}(T)$  model [1,3,4,7-9] to an independent set of high constraint ( $\approx$  SSV)  $K_{Jc}$  data. Equation 2 was used to adjust  $K_{Jc}$  to a reference  $K_{Jr}$  for  $B = 25.4$  mm. Another approach to evaluating  $[K_{Isy}/K_{Jc}]$  based on a self-calibrated Weibull stress statistical model gave very similar results [9].

The adjusted  $K_{Jr}$  for the B-W Shoreham matrix formed a very self-consistent data population with expected statistical properties and a  $T_o = -84\pm 5^\circ\text{C}$ . The adjustment procedure was also applied to the other UCSB Shoreham data, as well as a large set of  $K_{Jm}$  data for the same Shoreham plate section reported by Joyce and Tregoning, for a variety of standard specimens tested over a wide range of temperatures [3,8,9]. Remarkably, the entire Shoreham  $K_{Jr}$  database (445 data points) was well represented by a single MC with an ASTM E1921  $T_o = -85\pm 5^\circ\text{C}$ . Of course, the  $T_o$  of the individual subsets of data varied somewhat, but generally fell within the expected statistical distribution and only 22 of the 445 data points fell outside the 5 to 95% confidence interval.

#### **A $K_{Jm}$ Database for the IEA Heat of F82H and Adjustment to $K_{Jr}$**

The CL and SSV method described above were used to adjust the  $K_{Jm}$  IEA F82H database that we have assembled, currently composed of 219 data points. The  $K_{Jm}$  data represent a wide range of bend bar and compact tension specimen sizes from research programs at UCSB [10,11], ORNL [12], VTT [13] and NRG [14]. Figure 1 shows the  $K_{Jm}$  data that has been only adjusted for SSV size-effects based on Equation 2 to a reference  $B_r = 25.4$  mm,  $K_{Jmr}$ , based on the ASTM E1921 Standard; but these data have not been adjusted for CL effects. The MC and the 5 and 95% confidence interval curves based on a ASTM E1921 analysis of the  $K_{Jmr}$  data, that yielded a  $T_o \approx -119\pm 3^\circ\text{C}$ , are also shown. A large number of data points fall outside the 5 and 95% confidence interval; and at higher temperatures many fall below the 5% bound. Thus the  $K_{Jmr}$  data are not well represented by a single MC with  $T_o = -119^\circ\text{C}$ .

Figure 2 illustrates the strong effect of CL loss on the IEA F82H database. Here we plot the E1921  $T_o$  excluding  $K_{Jm}$  data with  $M$  below a variable censoring limit,  $M_{lim}$ , which has a nominal value of 30 in the ASTM Standard. Above  $M_{lim} \approx 200$  for the  $T_o$  plateaus at a SSV value of  $\approx -98\pm 5^\circ\text{C}$ . However,  $T_o$  decreases below a value of  $M_{lim} \approx 200$ , at a deformation level that is much lower at the E1921 limit of 30. Thus an E1921 analysis results in a highly non-conservative, small specimen  $T_o$  bias of  $\approx -21^\circ\text{C}$ .

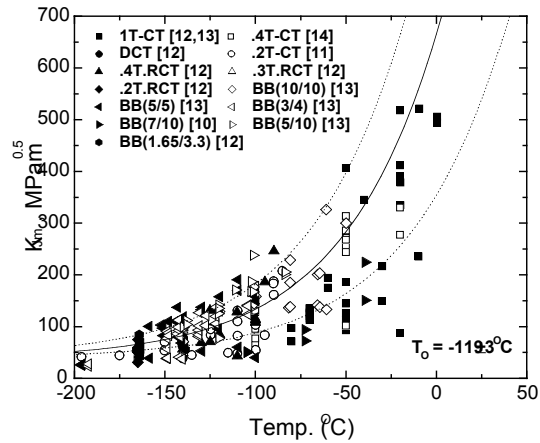


Figure 1. The F82H  $K_{Jmr}$  data versus temperature after a SSV (Equation 2) but with no CL adjustment and the median, 5% and 95% confidence interval toughness-temperature curves for the E1921  $T_0 = -119 \pm 3^\circ\text{C}$ .

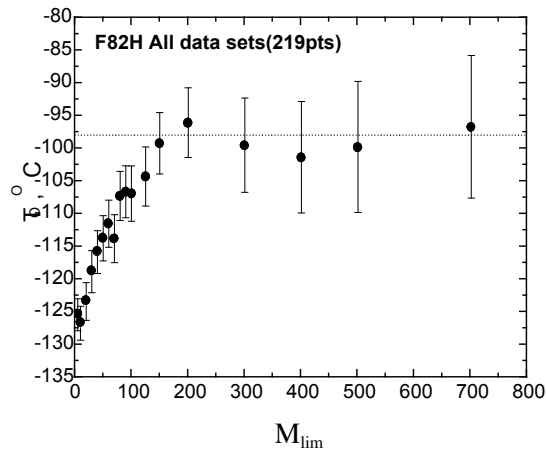


Figure 2. ASTM E1921 multiple temperature analysis  $T_0$  versus  $M_{lim}$  for the IEA F82H database, showing large effects of constraint loss and a SSY  $T_0 \approx 98 \pm 5^\circ\text{C}$  at  $M_{lim} > 200$ .

The CL adjustment procedure was calibrated to the IEA heat of F82H by fitting the  $K_{Jc}(T)$  model to a set of high constraint ( $\approx$  SSY) data based on a preliminary estimate of  $T_0 \approx -94^\circ\text{C}^{(1)}$ , yielding  $\sigma^* \approx 2100 \pm 100$  MPa for  $A^* = 2.5 \times 10^{-8} \text{ m}^2$ . The CL and SSV adjusted  $K_{Jr}$  data are shown in Figure 3, along with the corresponding MC and the 5 and 95% confidence interval curves based on a multiple-temperature ASTM E1921 analysis that yielded a  $T_0 \approx -103^\circ \pm 3^\circ\text{C}$ . This is reasonably consistent the best estimate  $T_0 = -98 \pm 5^\circ\text{C}$  based on the  $M_{lim}$  analysis, but reflects a slight residual small specimen bias that will be discussed below.

<sup>1</sup>Note the CL analysis was carried out prior to the multi-temperature  $T_0$  evaluation shown in Figure 3. The preliminary  $T_0 = -94^\circ\text{C}$  estimate was largely based on the results of data from the largest 1T CT specimens. Re-analysis based on  $\sigma^*$  for a  $T_0 = -98^\circ\text{C}$  would be possible, but this would not result in a significant change in the conclusions.

Figure 4 plots the differences between the adjusted  $K_{Jr}$  data and the MC median toughness,  $K_{Jo}$ , as a function of temperature for  $T_o = -98^\circ\text{C}$ . The MC 5 and 95% confidence interval curves are also shown, along with average  $K_{Jr} - K_{Jo}$ , and the corresponding standard deviations, in small intervals around common test temperatures. At lower temperatures the adjusted  $K_{Jr}$  data are slightly biased to the low side of  $K_{Jo}$ . This negative bias decreases at higher temperatures where the data become reasonably well centered, with the average deviations scattering about  $K_{Jr} - K_{Jo} = 0$ . However, a total of 34 data points fall below the nominal 5% and 22 above the 95% confidence interval limits, respectively. This is  $\approx 2.5$  times the number ( $\approx 22$ ) of data points expected to fall outside the 5 to 95% confidence interval. However, it is noted that most of these excess deviations are relative small.

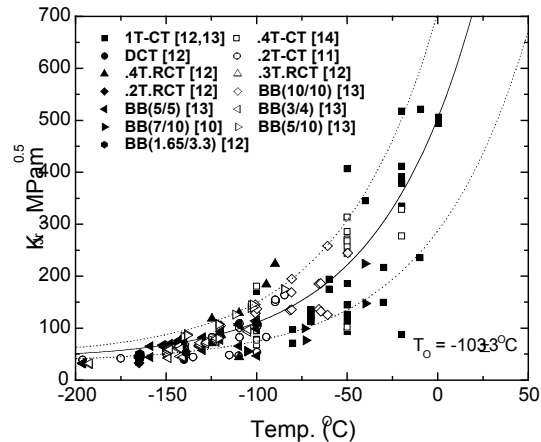


Figure 3. The F82H  $K_{Jr}$  data versus temperature after a SSV and CL adjustment and the median, 5% and 95% confidence interval toughness-temperature curves for the E1921  $T_o = -103 \pm 3^\circ\text{C}$ .

As highlighted by the arrows, examination of Figure 4 suggests that the CL and SSV model may slightly over-adjust the  $K_{Jm}$  data for very small specimen at low temperature and slightly under-adjust  $K_{Jm}$  at higher temperatures around and above  $T_o$ . This leads to a slightly lower  $T_o = -103^\circ\text{C}$  for the adjusted  $K_{Jr}$  database, compared to the  $T_o = -98^\circ\text{C}$  found in the  $M_{lim}$  analysis. This is not surprising, since in bending dominated crack tip fields, the  $[K_{I,ssy}/K_{ssy}]$  adjustments are larger at lower  $\sigma^*/\sigma_y$ . Since  $\sigma_y$  increases with decreasing temperature,  $\sigma^*/\sigma_y$  decreases. Thus the model may tend to over-adjust the measured data at low temperature and under-adjust at the higher temperatures. In addition, the applicability of SSV adjustments of low temperature data is questionable; indeed, SSV adjustments of data near or on the lower shelf regime are not recommended in the E1921. Further, this assessment assumes that the shape and lower shelf toughness of the MC described by Equation 1 is precisely applicable to TMS, which may not be the case. Other issues that are not completely resolved relate to the physical basis for and value of  $K_{min} = 20 \text{ MPa}\sqrt{\text{m}}$ , and assumptions leading the nominal confidence limits specified in the E1921 Standard. Finally, the excess scatter may in part be due to material heterogeneity for different IEA F82H plate sections and section thicknesses or thickness locations. Such heterogeneity may have the largest impact on the 25.4 mm specimens, with a full through-plate thickness crack, that may sample the lowest toughness microstructure at the center-plane of the plate. We plan to carry out additional research directly aimed at resolving these issues.

However, the issue of possible excess scatter aside, it is clear that the adjusted  $K_{Jr}$  data are in generally good agreement with a single MC with  $T_o = -98 \pm 5^\circ\text{C}$  MC. Thus there can be considerable confidence in  $\sigma T_o$  evaluations, including for irradiation embrittlement, based on the MC- $\sigma T$  method using a sufficient number of small specimens, provided that size effects are properly accounted for. However, assessing the  $\sigma T_o$  for irradiation embrittlement raises some additional issues. First, the effect of reduced strain hardening on increased CL in irradiated specimens must be carefully quantified. Second, while results to

date are promising [6], the effects of irradiation on the shape of the MC for large  $\sigma_y$  and  $T_o$  are not fully understood.

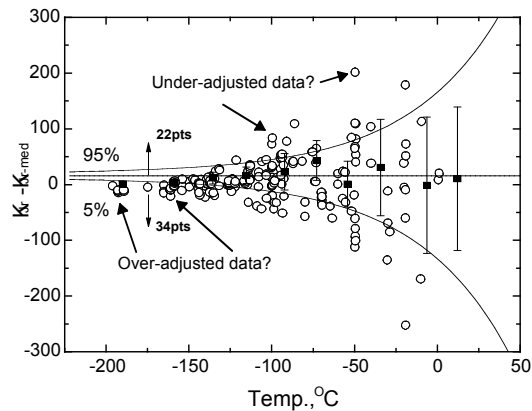


Figure 4.  $K_{Jr} - K_{J0}$  as a function of temperature and the corresponding 5 and 95% confidence interval curves for  $T_o = -98^\circ\text{C}$ . The square symbols and error bars are the average and one standard deviation  $K_{Jr} - K_{J0}$  for groups of data over small test temperature intervals. The arrows indicate data that may be under-adjusted leading to a slightly lower  $T_o = -103^\circ\text{C}$ .

### Summary and Conclusions

We have assembled a database on the fracture toughness of the IEA heat of F82H. The database, currently composed of 219 data points, is based a wide variety of compact tension and bend bar specimen sizes. ASTM E1921 evaluation of this database yielded a  $T_o = -119 \pm 3^\circ\text{C}$ . However, the data are not well represented by a single MC. In the past, these deviations have raised questions about the applicability of the MC based methods to TMS, or were attributed to material heterogeneity.

However,  $T_o$  is sensitive to the assumed deformation limit,  $M_{lim}$ , specified in E1921 as 30; and  $T_o$  decreases systematically with decreasing  $M_{lim}$  starting at a much higher value  $\approx 200$  due to constraint loss. At higher  $M_{lim} > 200$ ,  $T_o$  reaches a SSY plateau of  $\approx 98 \pm 5^\circ\text{C}$ . Thus we applied a calibrated size-adjustment procedure, which accounts for constraint loss effects that are controlled by the specimen size, as well as statistical effects of B. An E1921 analysis of the fully adjusted toughness database gave a  $T_o = 103 \pm 4^\circ\text{C}$ , close to the result of the  $M_{lim}$  analysis; and the adjusted  $K_{Jr}$  data are in reasonably good agreement with a MC with  $T_o = -98^\circ\text{C}$ . However, the scatter was somewhat larger than predicted, with  $\approx 25\%$  of the data points falling outside the estimated 5 to 95% confidence interval. Nevertheless, the excess deviations were generally small and can in part be linked to the approximate adjustment model. The data generally seemed to be slightly over-adjusted at very low temperatures and slightly under-adjusted at temperatures around  $T_o$  and above. Finally, we describe a number of issues that are not fully resolved, including possible excess scatter. However, the results of this study lend strong support to the use of MC-type methods in characterizing the effects of irradiation and other variables on the toughness temperature curves of TMS.

### Future Research

We will continue to add and analyze additional data on the IEA F82H as it becomes available. We will also extend the database to include other  $\approx 8\text{Cr}$  TMS including Eurofer98 and irradiated alloys. Experiments aimed at resolving the various issues noted in the previous section.

## Acknowledgements

This research was supported by the DOE Office of Fusion Energy Science (Grant # DE-FG03-94ER54275). The authors also explicitly acknowledge the large IEA F82H database developed by Dr. K. Wallin of VTT Laboratory in Finland.

## References

- [1] G. R. Odette, K. Edsinger, G. E. Lucas, and E. Donahue, *Small Specimen Test Techniques*, V3, ASTM STP 1329, American Society for Testing and Materials (1998) 298.
- [2] ASTM E 1921-03, Standard Test Method for Determination of Reference Temperature,  $T_0$ , for Ferritic Steels in the Transition Range, *Annual Book of ASTM Standards: Metals Mechanical Testing; Elevated and Low Temperature Tests; Metallography*, V03.01, American Society for Testing and Materials (2003).
- [3] G. R. Odette, T. Yamamoto, H. J. Rathbun, M. L. Hribernik, and J. W. Rensman, *J. Nucl. Mater.* 323 (2003) 313.
- [4] G. R. Odette and M. Y. He, *J. Nucl. Mater.* 283-287 (2000) 120.
- [5] G. R. Odette and M. Y. He, *J. Nucl. Mater.* 307-311 (2002) 1624
- [6] G. R. Odette, H. J. Rathbun, J. W. Rensman, and F. P. van den Broek, *J. Nucl. Mater.* 307-311 (2002) 1011.
- [7] H. J. Rathbun, G. R. Odette, and M. Y. He, *Proceedings of the International Congress on Fracture 10* (2001) (searchable Elsevier CD format).
- [8] H. J. Rathbun, G. R. Odette, M. Y. He, T. Yamamoto, and G. E. Lucas, *Applications of Fracture Mechanics in Failure Assessment*, PVP 462, American Society of Mechanical Engineers (2003) 31.
- [9] H. J. Rathbun, G. R. Odette, M. Y. He, G. E. Lucas, and T. Yamamoto, *Size Scaling of Cleavage Toughness in the Transition: A Single Variable Experiment and Model Based Analysis*, NUREG/CR 6790, U.S. Nuclear Regulatory Commission (2004) in press.
- [10] P. Spatig, G. R. Odette, E. Donahue, and G. E. Lucas, *J. Nucl. Mater.* 283-287 (2000) 120.
- [11] P. Spatig, E. Donahue, G. R. Odette, G. E. Lucas, and M. Victoria, *Multiscale Modeling of Materials 2000*, MRS Symposium Proceedings 653, Materials Research Society (2001) Z7.8.
- [12] M. Sokolov, R. Klueh, G. R. Odette, K. Shiba, and H. Tanaigawa, *Effects of Irradiation on Materials – 21st International Symposium*, ASTM STP 1447, American Society for Testing and Materials (in press) and private communication.
- [13] K. Wallin, A. Laukkanen, and S. Tahtinen, *Small Specimen Test Techniques*, V4, ASTM STP 1418, American Society for Testing and Materials (2002) 33.
- [14] J.-W. Rensman et al., *J. Nucl. Mater.* 307–311 (2002) 245.